4038

Electric Birefringence of Bacterial Flagellar Protein Filaments : Evidence for Field-induced Interactions

BERNARD R. GERBER, AKIRA MINAKATA AND LEO D. KAHN

Electric Birefringence of Bacterial Flagellar Protein Filaments: Evidence for Field-induced Interactions

BERNARD R. GERBER, AKIRA MINAKATA†

Department of Biology, University of Pennsylvania
Philadelphia, Pa. 19174, U.S.A.

AND

LEO D. KAHN

ARS. United States Department of Agriculture
Philadelphia, Pa. 19118, U.S.A.

The time course for the build-up and decay of birefringence induced by a rectangular voltage pulse was measured on solutions of flagellar filaments from *Salmonella equi-abortus* (strain SJ25). These filaments are tubular polymers of protein (degree of polymerization $\approx 10^3$) constituted by non-covalent linkage of flagellin monomers of molecular weight 4×10^4. The effect on electro-optical properties of solutions of filaments due to variations in temperature, concentration and mean length of protein filaments, and the duration and intensity of the applied electric field is described. Analysis of the field intensity dependence of the birefringence and comparison of the build-up and decay processes indicate that orientation in the field is due primarily to the existence of a permanent dipole moment in the filaments. At 18°C the following values were obtained for a solution of filaments with mean length and standard deviation of 0·39 and 0·30 μm: specific Kerr constant $(K_{sp}) = 6{\cdot}14\times10^{-3}$ electrostatic units; optical anisotropy factor $(g_1 - g_2) = 5{\cdot}66\times10^{-3}$; dipole moment $(\mu) = 1{\cdot}01\times10^5$ Debye units; and mean relaxation time $(\bar{\tau}) = 9{\cdot}20$ ms. At temperatures below 20°C there is a marked increase in the optical anisotropy factor of the filaments which may be due to a change in their flexibility. The large values of K_{sp} obtained indicate the highly responsive nature of these filaments to an electric field. The birefringence decay curves were decomposed by computer into a specified number of exponential terms from which both the mean length and the size distribution of these polydisperse filaments were calculated. The results obtained were in substantial agreement with the values of these parameters observed by electron microscopy. A cumulative field effect dependent on field intensity and filament concentration was observed. Repeated pulsing of electric field, above threshold values of field intensity and filament concentration, produced decreases in the birefringence near 60% of its initial value. The effect was reversible with a time constant greater than two minutes. No appreciable change in the relaxation time for decay of birefringence was observed on multiple pulsing of these solutions. These results are interpreted consistently to arise from the sidewise aggregation of filaments induced by electrical impulses of sufficient intensity and duration. These properties appear relevant to bacterial motility: variations in electric potential along the membrane of the bacterium might serve first to orient these

† Present address: Department of Physics, Faculty of Science, Nagoya University, Nagoya, Japan.

organelles and then to induce their coalescence to "bundles" of filaments. The latter structures are commonly observed *in vivo*. In this way the activity of flagella might be co-ordinated.

1. Introduction

The bacterial flagellar filament is a tubular polymer of proteins joined through non-covalent bonds. This polymer has served well as a model self-assembly system (Kushner, 1969; Iino, 1969; Asakura, 1970). Agents such as elevated temperature or pressure, high and low pH, detergents, urea and guanidine will dissociate the filaments into their constituent protomers, the flagellins. On removal of the agent the flagellins may reassociate to form tubules that are virtually identical to the original ones. As emphasized so excellently in a review article by Holtzman (1974), a full understanding of the mechanism of reversible self-assembly is of fundamental importance to so many areas in the biomedical sciences, particularly to the fields of developmental biology and cellular motility.

Aspects of the mechanism of flagellin assembly were described in detail in a recent study of the kinetics and thermodynamics of the process (Gerber *et al.*, 1973). The self-assembly of flagellin was shown to be endothermic, i.e. an entropy-driven reaction which occurred as a phase transition. At equilibrium, the conditions of temperature and solvent composition defined a monomer concentration, similar to a critical micelle concentration, that could co-exist with *any* concentration of polymer.

The physical basis for the high specificity involved in these protein–protein interactions was sought in a study of the dielectric behavior of monomers and polymers of flagellar filament protein (Gerber *et al.*, 1972). Though other proteins were found to have dipole moments less than 400 Debye units, proteins which self-assembled were found to have *permanent* dipole moments greater than 700 Debye units. Moreover, on polymerizing to tubular filaments, the dipole moment per monomer in a filament decreased markedly in conformity with a principal of dipole neutralization.

Despite the relative success of the dielectric method, however, technical difficulties prevented a complete study on polymers of flagellar protein. For example, the critical frequency for dielectric dispersion of polymers ($\bar{L} = 0{\cdot}17$ μm) occurred at a frequency near 1 kHz. Measurements of dielectric constant and conductivity of solutions at such low frequencies required specially designed equipment and techniques (Schwan, 1963). Alternatively, the technique of electric birefringence (O'Konski & Haltner, 1956,1957; Yoshioka & Watanabe, 1969; Kahn, 1972) is particularly well-suited to measurements on polymer solutions and, in addition, requires only 0·3 ml of solution at solute concentrations below 1 mg/ml. By this procedure, measurements are made of the rate and extent of orientation of molecules in response to a pulsed electric field. Analysis of the build-up of birefringence following establishment of the field, and the decay of birefringence after the pulse is terminated, results in information on the size and shape of the molecules as well as the nature and magnitude of their dipoles.

This report describes an application and extension of the electric birefringence method to the study of bacterial flagellar filaments. The effect of variations in temperature, concentration and mean length of protein filaments and the duration and intensity of the applied electric field is described. In addition, a method is introduced to obtain the size distribution of a polydisperse solution of filaments from birefringence decay curves. The results obtained are in substantial agreement with the

single rectangular-wave pulse of an electric field, adjustable in duration (1·5 ms to 12 ms used) and intensity (0·235 to 4·45 kV/cm used), was applied across the cell. The transient birefringence induced by the field was detected as variations in potential across the photomultiplier load. Calibration curves, made separately, were used to relate values of photomultiplier potential to angular rotations of the analyzer prism and the birefringence of the sample solution.

Output signals from both the pulse generator and photomultiplier were displayed on a dual trace storage oscilloscope (Tektronix model 549 with 1A1 accessory). Traces remained visible on the screen until released by a pushbutton switch. These were subsequently photographed with a Hewlett Packard camera (model 197A) using Polaroid 107 film.

Measurements of birefringence were made in a range which permitted a reproducibility of better than $\pm 2\%$. At field intensities above 1 kV/cm a decrease in electric birefringence was observed when samples were treated with multiple pulses of electric fields. Therefore, unless specified to the contrary, each result represents data obtained on a fresh sample which previously had never been pulsed by electric fields.

(h) *Analysis of data*

The birefringence of a solution and the applied pulse *versus* time were recorded as dual traces on the oscilloscope. These oscillograms were converted to values of birefringence and automatically digitized with an optical scanning device using a television camera and controlled by computer (PDP-10, Digital Equipment Corp., Maynard, Mass.). Plainly erroneous points, such as those arising from confusion between the experimental curve and grid lines of the oscilloscope, could be edited from the digitized data. Under optimal conditions a maximum of 100 data points could be obtained to represent a single experimental curve. Digitized data subsequently were decomposed to a specified number of exponential terms by a non-linear optimization routine based on a steepest descent method devised by Professor Martin Pring (unpublished work). This procedure seeks a minimum value for the mean-square deviation between digitized (experimental) and calculated (decomposed) points. To provide a permanent record, experimental and calculated data were printed and also displayed on an X–Y plotter (Calcomp model 565, California Computer Products, Inc.). The programs used permitted rescanning of pictures and reanalysis of data.

(i) *Calculations of molecular parameters*

The electric birefringence of a solution Δn is defined as

$$\Delta n = n_{\parallel} - n_{\perp}\,, \tag{1}$$

where $n_{\parallel}$ and $n_{\perp}$ are the indices of refraction of a sample to plane polarized light in a direction parallel to, and perpendicular to, an applied electric field.

For a dilute solution of axially symmetrical particles, Δn was given by Peterlin & Stuart (1939) as equivalent to

$$\Delta n = (2\pi C_v/n)\,(g_1 - g_2)\phi\,. \tag{2}$$

In equation (2) n is the refractive index of the solution, C_v the volume fraction of the solute, $(g_1 - g_2)$ the optical anisotropy factor, ϕ the orientation factor and the subscripts 1 and 2 refer to longitudinal and transverse axes of the particle. At high field intensity $\phi \to 1$ and consequently the saturation birefringence Δn_s is given by

$$\Delta n_s = (2\pi C_v/n)\,(g_1 - g_2)\,. \tag{3}$$

From equations (2) and (3) it is apparent that

$$\phi = \Delta n/\Delta n_s\,. \tag{4}$$

At low field intensity Δn is proportional to the square of the field intensity, and a specific Kerr constant, K_{sp} (Peterlin & Stuart, 1939; O'Konski *et al.*, 1959), can be defined as

$$\begin{aligned} K_{sp} &= (C_v n)^{-1}\,(\Delta n/E^2)_{E\to 0} \\ &= (2\pi/15n^2)\,(g_1 - g_2)\,(b^2 + 2c)\,. \end{aligned} \tag{5}$$

In equation (5) E is field intensity, $b = \mu/kT$, $c = (a_1 - a_2)/2kT$, where μ is the permanent dipole moment along the longitudinal axis of the molecule, k is the Boltzmann constant, T is the absolute temperature and $(a_1 - a_2)$ is the electrical polarizability anisotropy of the molecules in the solvent. Combining equations (2) and (5) then leads to the expression

$$(\Delta n/E^2)/(\Delta n/E^2)_{E\to 0} = 15\phi(\beta,\gamma)/(\beta^2 + 2\gamma)\,, \tag{6}$$

where $\beta = bE$, $\gamma = cE^2$ and ϕ is a function of β and γ (O'Konski *et al.*, 1959). The right-hand side of equation (6) has been evaluated as a function of $(\beta^2 + 2\gamma)$ for various ratios of $\beta^2/2\gamma$ (O'Konski *et al.*, 1959), whereas the quotient on the left-hand side is an experimentally determined quantity. Values of b and c can be obtained by comparing the graph of $(\Delta n/E^2)/(\Delta n/E^2)_{E\to 0}$ *versus* $\log(E^2)$ with graphs of $15\phi(\beta,\gamma)/(\beta^2 + 2\gamma)$ *versus* $\log(\beta^2 + 2\gamma)$. The abscissa of the latter is equal to $\log(b^2 + 2c) + \log(E^2)$, and curves have been calculated for various values of $b^2/2c(= \beta^2/2\gamma)$.

In addition, $(b^2 + 2c)$ can be determined from experimental quantities by substituting equation (3) into (5) so that

$$(b^2 + 2c) = (15/\Delta n_s)\,(\Delta n/E^2)_{E\to 0}\,. \tag{7}$$

For limiting high field intensities and molecular orientation due primarily to a permanent dipole moment ($\beta^2 \gg \gamma$), the orientation factor ϕ has been given by O'Konski and coworkers (1959) as

$$\phi(\beta,0) = 1 - 3/\beta + 3/\beta^2\,. \tag{8}$$

This equation proves useful in evaluating the dipole moment of a molecule which possesses only a permanent moment.

Benoit (1951) derived the following expressions for the time course of rise and decay birefringences, under the action of a rectangular voltage pulse, at limiting low field intensities:

$$\frac{\Delta n(t)}{\Delta n(\infty)} = 1 - \frac{3r}{2(r+1)}\exp(-2Dt) + \frac{r-2}{2(r+1)}\exp(-6Dt) \tag{9}$$

$$\frac{\Delta n(t)}{\Delta n(0)} = \exp(-6Dt)\,. \tag{10}$$

In equations (9) and (10) r is $b^2/2c$, the rotary diffusion constant D is defined as $(6\tau)^{-1}$, where τ is the relaxation time, and $\Delta n(\infty)$ in the rise curve (depicted as region II, Plate II(b)) is equal to $\Delta n(0)$ in the decay curve (region III) for a sufficiently long pulse, t is either build up or decay time. From these equations Yoshioka & Watanabe (1969) obtained the following expression with $\Delta n(\infty) = \Delta n(0) = \Delta n_0$:

$$\frac{A_1}{A_2} = \frac{\int_0^\infty [1 - \Delta n(t)/\Delta n_0]\mathrm{d}t}{\int_0^\infty [\Delta n(t)/\Delta n_0]\mathrm{d}t} = \frac{4r+1}{r+1}\,. \tag{11}$$

The numerator in equation (11) corresponds to the area A_1 between the rise curve and the line $\Delta n(t)/\Delta n_0 = 1$, and the denominator the area A_2 between the decay curve and $\Delta n(t)/\Delta n_0 = 0$. The ratio of the two areas approaches 4 for a molecule with $\gamma/\beta^2 \to 0$ or, more exactly, $4 - (13/42)\beta^2$.

For limiting high field intensities and permanent dipole moment orientation, the rise curve has been expressed by O'Konski *et al.* (1959) as

$$\frac{\Delta n(t)}{\Delta n(\infty)} = 1 + \frac{12y}{(y-1)^2} - \frac{6xy(y+1)}{(y-1)^3}\,, \tag{12}$$

where

$$x = 2\beta Dt; \qquad y = \exp(x)\,. \tag{13}$$

Equation (12) gives a value of 3·31 for x when $\Delta n(t)/\Delta n(\infty) = 1 - \mathrm{e}^{-1}$. From equation (13) an apparent time constant of the rise curve τ_R can be defined as

$$\tau_R = 3{\cdot}31/2\beta D\,. \tag{14}$$

By inserting $\tau_D = (6D)^{-1}$, equation (14) reduces to

$$\beta = 9{\cdot}94\tau_D/\tau_R \,. \tag{15}$$

(Subscripts D and R refer to parameters associated with decay and rise birefringence processes.) Equation (15) provides still another method for determining the dipole moment of a molecule for the case of permanent dipole moment orientation at high electric field intensities.

For a polydisperse solution, the decay of birefringence and the average relaxation time are (Matsumoto *et al.*, 1970)

$$\Delta n(t) = \sum_i \Delta n_i(0) \exp(-t/\tau_i) \tag{16}$$

$$\bar{\tau} = \sum_i \tau_i \Delta n_i(0)/\Delta n(0) \,, \tag{17}$$

where $\Delta n(0) = \Sigma_i \, \Delta n_i(0)$ and i refers to the molecular species with relaxation time τ_i.

For highly elongated molecules $(g_1 - g_2)$ is known to be independent of the length of the molecules (Peterlin & Stuart, 1939), and the orientation factor ϕ is proportional to the square of the length of the molecules for low field intensities, and has the value of unity for limiting high field intensities. The volume fraction of the molecules C_v is expressed as

$$C_v = \bar{v} \nu_i l_i \,, \tag{18}$$

where $\bar{v}$ is the partial specific volume of the molecules, ν_i is the number of molecules of species i with length l_i. On substitution of $\tau_i = (6D_i)^{-1}$, Perrin's equation (Perrin, 1934) for the rotary diffusion constant D of a prolate ellipsoid of revolution with axial ratio p_i in a solvent with viscosity η rearranges to

$$\tau_i = \frac{\pi \eta l_i^3}{9kT(2 \ln(2p_i) - 1)} \,. \tag{19}$$

For low field intensities this becomes

$$\bar{\tau} = \frac{\pi\eta}{9kT} \frac{\sum_i \nu_i l_i^6 [2 \ln(2p_i) - 1]^{-1}}{\sum_i \nu_i l_i^3} \,. \tag{20}$$

For high field intensities

$$\bar{\tau} = \frac{\pi\eta}{9kT} \frac{\sum_i \nu_i l_i^4 [2 \ln(2p_i) - 1]^{-1}}{\sum_i \nu_i l_i} \,. \tag{21}$$

Equation (20) corresponds to a $(Z + 1)$ average value of τ, whereas (21) corresponds to a weight average value of $\bar{\tau}$. These last two equations were used in comparing the values of $\bar{\tau}$ observed in electronic birefringence measurements with those obtained for the length distribution of flagellar filaments by electron microscopy.

(j) *Protein concentration*

The opalescence of solutions varied between samples of flagellar filaments. Therefore, analysis by ultraviolet absorbance for the concentration of this protein in solution was unreliable. Preferably, the Biuret test of Gornall *et al.* (1949) was used. The alkalinity of the test reagent caused the filaments to dissociate to clear solutions of monomers making light-scattering corrections unnecessary. Using bovine serum albumin as a standard, absorbance at 540 nm above a solvent plus reagent blank was found to be proportional to concentration in the range 1 to 8 mg/ml protein with slope 0·049 per mg/ml protein.

3. Results

(a) *Electric birefringence patterns*

An oscillogram produced in a typical electric birefringence experiment on flagellar filaments is shown in Plate II(a). The upper trace in the Plate shows the duration

and amplitude of a single rectangular voltage pulse; the lower one shows the optic response of the sample.

Features of the birefringence pattern to be used in subsequent analyses are illustrated in separate regions in Plate II(b). Region I shows the build-up of birefringence of the protein solution in response to the applied electric field. The shape of the rise curve contains information on the mechanism for orienting molecules in the electric field and the relative contribution of induced and permanent dipoles. The condition of steady-state birefringence for the solution occurs in region II. In this region the molecules are aligned in the electric field to an extent determined by such factors as the field intensity, temperature, charge distribution and polarizability of the molecules. Region III contains the birefringence decay process which occurs after the field has been terminated. The decay of birefringence yields dimensions for an appropriate hydrodynamic model and an estimate of the polydispersity of the sample.

(b) *Effect of field intensity on* Δn

The steady-state birefringence (Δn) of flagellar filaments (0·39 mg/ml) was determined at 18°C and at various field intensities. Δn is plotted against the square of the field intensity in Figure 2. A marked decrease in the slope of the curve is apparent at field intensities above 1·4 kV/cm. Consequently, the value obtained at the highest field intensity measured, 4·45 kV/cm, is close to the value representing full saturation of birefringence.

The graph in the insert to Figure 2, which places emphasis on values of Δn obtained at low field intensities, indicates that there is no measurable linear region and the results deviate from the Kerr law. Inserting the value for the limiting slope of the curve, $(\Delta n/E^2)_{E\to 0}$, into equation (5) and taking the specific volume as 0·73 cm^3/g (Gerber & Noguchi, 1967), expressing the concentration as the volume fraction C_v and $n = 1{\cdot}333$, the specific Kerr constant K_{sp} for flagellar filaments is $6{\cdot}14\times10^{-3}$ e.s.u.

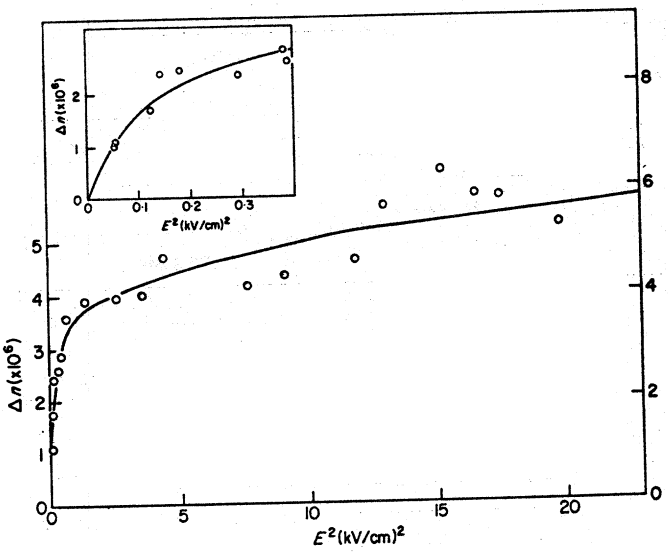

FIG. 2. Dependence of electric birefringence at steady state of short polymers on the square of the field intensity at 18·0°C. Filament concentration was 0·39 mg/ml. Insert to the Figure is an enlargement of values observed at low field intensities.

PLATE I. Electron micrographs of *Salmonella equi-abortus* SJ25 with flagella intact, isolated flagellar filaments and fragments of filaments. Specimens were suspended in distilled water and negative stained with potassium phosphotungstate (2%, w/v), pH 7·0. Bar = 1 μm.

(a) Bacterium with 15 wavy peritrichous flagella. Electron microscope grid was photographed at a magnification of 2800×.

(b) Purified sample of SJ25 flagellar filaments (long polymers). Filaments are polydisperse with respective mean values for contour and end-to-end lengths of 0·90 and 0·82 μm. Longer filaments have prounced curvature. Grid was photographed at a magnification of 4540×.

(c) Fragments of SJ25 flagellar filaments (short polymers) made by ultrasonication of the sample in (b). Fragments are polydisperse with mean values for contour and end-to-end lengths of $0{\cdot}39_5$ and $0{\cdot}38_8$ μm. The shorter fragments are straight or slightly curved rods. Grid was photographed at a magnification of 4560×.

PLATE I.

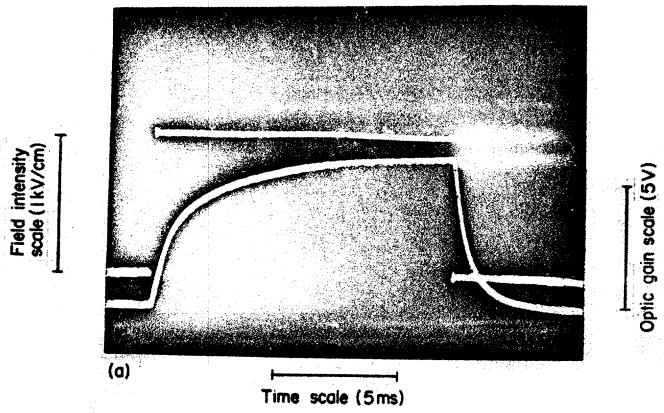

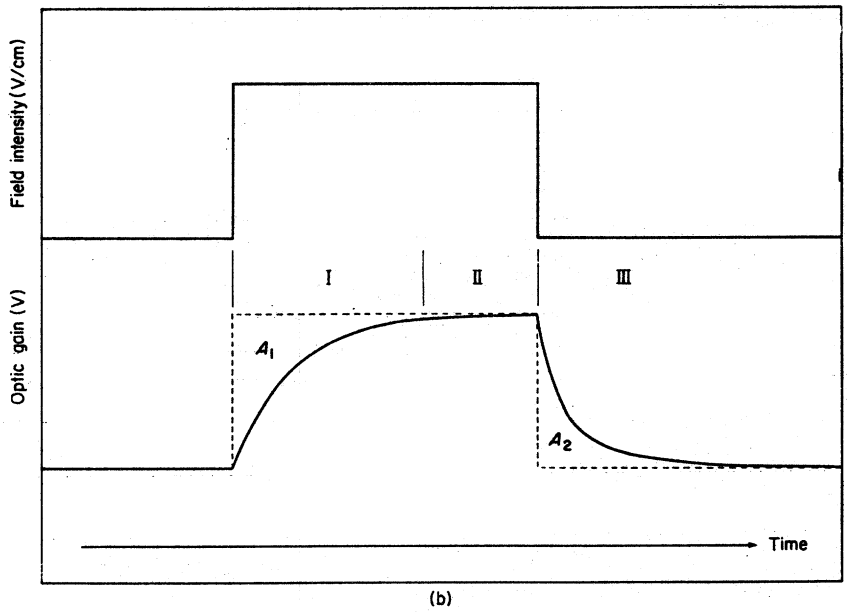

PLATE II. (a) Typical oscilloscope traces for optic response of short polymers of flagellar filaments produced by an applied voltage pulse. Filament concentration was 3·08 mg/ml. Electric field intensity and pulse duration were 1·02 kV/cm and 12 ms. Temperature, 25·9°C. Buildup in birefringence was slower than its decay.

(b) Schematic illustration of dual trace oscilloscope pattern. The upper trace is the variation with time of an applied rectangular electric pulse. The lower trace is the optic response curve of the sample. Labels in the illustration refer to buildup (region I), steady state (region II) and decay (region III) of the optic response. After conversion from voltage to birefringence terms the ratios of areas between the optic response curve and the broken lines A_1/A_2 can be related to the polarization mechanism. $A_1/A_2 = 1$ for orientation due only to an induced dipole moment of the sample; $A_1/A_2 \to 4$ for molecular orientation due only to a permanent dipole moment.

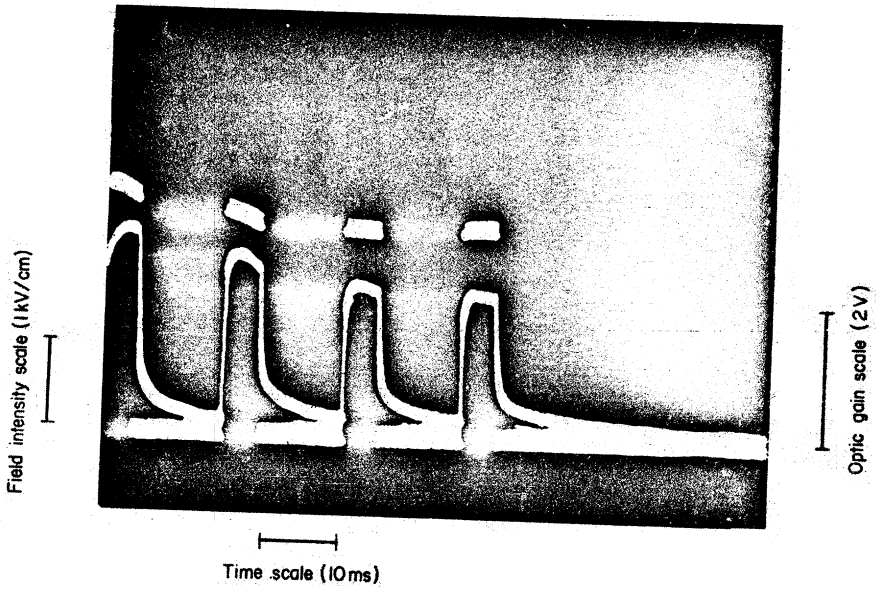

PLATE III. Oscillogram showing optic response of a solution of short polymers to a train of four voltage pulses. Protein concentration, 0·39 mg/ml; temperature, 18°C; applied field intensity varied from first to last pulse between 2·79 and 2·38 kv/cm; pulse duration and interval between pulses were 5 and 11 ms.

(c) *Effect of protein concentration on* Δn

At a field intensity of 1·6 kV/cm, the effect of protein concentration on the steady-state birefringence of short and long polymers of flagellar filaments was determined (Fig. 3). Values of Δn are linearly related to concentration for short polymers (curve A) but are non-linear for long polymers (curve B). Due to the lack of direct proportionality between Δn and concentration for long polymers, indicative of filament–filament interactions in solution, subsequent studies were limited primarily to measurements on short polymers.

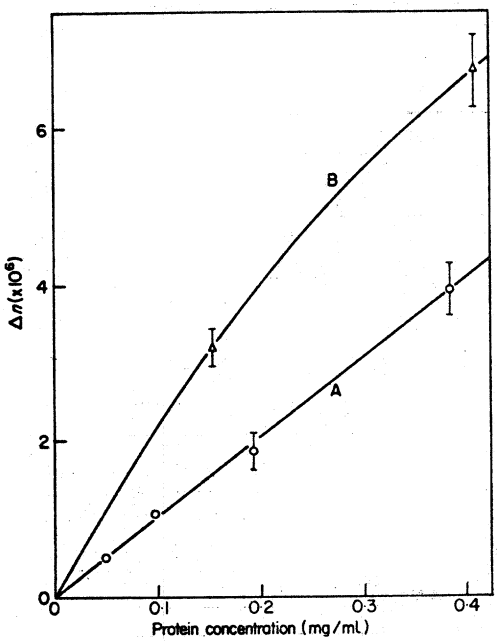

FIG. 3. Effect of protein concentration on Δn produced by an applied field of 1·6 kV/cm. Curve A, short polymers of flagellar filaments at 18°C; curve B, long polymers of filaments at 26°C.

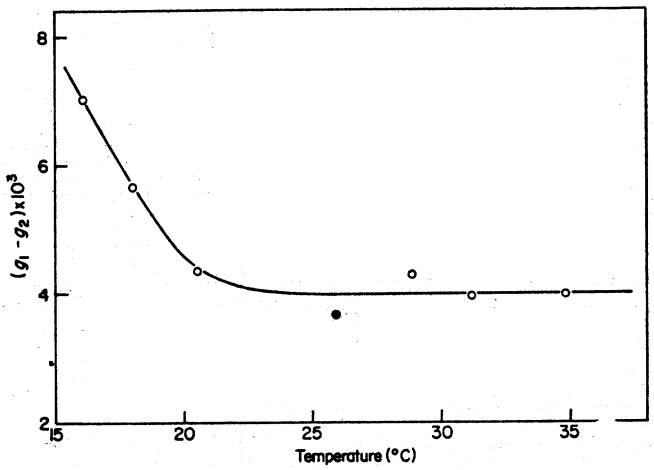

FIG. 4. The effect of temperature on $(g_1 - g_2)$ of short polymers. Protein concentrations, 0·39 (○) and 3·08 (●) mg/ml.

(d) *Optical anisotropy factor*

The saturation birefringence Δn_s, defined as $\Delta n_{E\to\infty}$, was obtained from the intercept with the ordinate in a graph of Δn against E^{-2}. At high field intensity where equation (3) is valid, values of Δn_s can be readily converted to values of $(g_1 - g_2)$, the optical anisotropy factor. The effect of temperature on the latter is shown in Figure 4. At temperatures above 20°C, $(g_1 - g_2)$ is independent of temperature and has a value of $4{\cdot}07\ (\pm 0{\cdot}25) \times 10^{-3}$. As expected, values obtained for $(g_1 - g_2)$ above 20°C appeared independent of filament concentration. An eightfold increase in concentration, represented by the filled circle in Figure 4, caused no appreciable change in $(g_1 - g_2)$. With decrease in temperature below 20°C, the optical anisotropy factor increased and had a value of $7{\cdot}02 \times 10^{-3}$ at 16·1°C. We interpret this result to indicate an increase in flexibility of the filament with increase in temperature (see Discussion).

(e) *Decay of birefringence*

(i) *Computer simulations*

In preliminary analyses of data it was found that graphs of log Δn *versus* time after the electric field was quenched (region III in Plate II(b)) were non-linear, which indicated the existence of a distribution of relaxation times and hence a polydisperse sample. Therefore, as described in Materials and Methods, the data were automatically digitized and decomposed by computer into various numbers of exponential terms.

It is well known that computer simulations of data are replete with difficulties and that on occasion physically meaningless solutions may be produced. Accordingly,

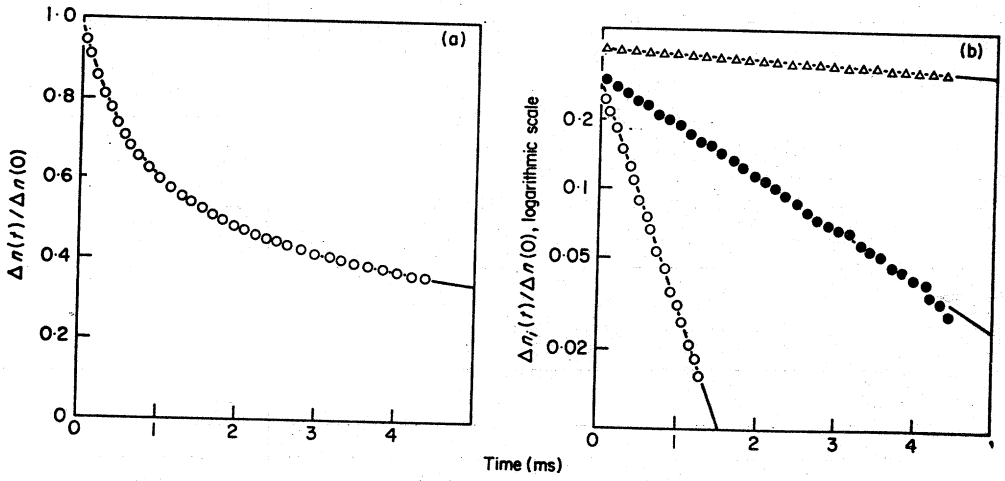

FIG. 5. (a) Computer simulation of an observed electric birefringence decay process for short polymers at 18·0°C. Applied field intensity and pulse duration were 545 V/cm and 12 ms. Protein concentration, 0·39 mg/ml. Zero time for the decay process is the instant when the electric pulse was terminated. Circles are digitized data and the curve is the computed sum of three exponential terms which minimizes the least-squares deviation.

(b) Semilogarithmic graph of data in (a) decomposed by computer to three terms. The intercepts with the ordinate give the contribution to the birefringence of each of the three terms. Points are calculated and connected with a least-squares line. Relative contributions and apparent relaxation times for the terms are —△—△—, 0·405 and 19·4 ms; —●—●—, 0·309 and 1·96 ms; —○—○—, 0·286 and 0·447 ms.

several criteria were adopted to define an acceptable fit to data. First, we required that contributions of all terms be positive; solutions with terms having negative contributions were excluded from consideration. Second, solutions with terms having contributions less than 5% of the total were thought to have little significance since approximately the same solution could be obtained on omitting these terms. Finally the mean-square deviation between calculated and experimental data had to be less than 0·5.

In Figure 5(a) is shown output from the growth plotter of a computer simulation where 99 digitized data points were decomposed into three terms. For ease in calculation the ordinate is normalized to unity and represents the fraction of birefringence remaining at any instant after the electric field is released. In the Figure, circles represent one third of the digitized data and the line represents the calculated best fit to the data of the sum of three exponential terms. The time course for each of the three components and their relative contributions are indicated in the semi-logarithmic plots in Figure 5(b). The relaxation time for each term was evaluated from the slope of the line in Figure 5(b) according to equation (10). The average relaxation time $\bar{\tau}$ was calculated from equation (17) and had a value of 9·2 ms. Table 1 compares values of $\bar{\tau}$ obtained when the number of terms used to represent the data was varied. The relative contribution and relaxation time for each computer solution, up to four-term decompositions, are tabulated in Table 1. It has not been possible to decompose data into five terms with any degree of consistency. As the number of decomposed terms increases $\bar{\tau}$ also increases since components with longer relaxation times are isolated in succession.

TABLE 1

Number of computed terms for the birefringence decay process and the mean relaxation time $\bar{\tau}$ of short polymers at 18·0°C†

Number of decompositions by computer	τ_i‡ (ms)	Relative contribution‡ (%)	$\bar{\tau}$§ (ms)	s‖
2	0·476	36·6		
	5·81	63·4		
			3·86	0·663
3	0·152	12·3		
	1·06	41·1		
	10·4	46·6		
			5·30	0·196
4	0·114	9·3		
	0·800	34·0		
	4·00	31·4		
	20·0	25·3		
			6·60	0·189

† Protein concentration, 0·39 mg/ml; intensity and duration of the applied electric field were 4·16 kV/cm and 3·8 ms; number of digitized points, 99.

‡ Calculated with the use of equation (16).

§ Calculated with the use of equation (17).

‖ Root-mean-square deviation between digitized and computed data points.

(ii) *Effect of temperature and field intensity on* $\bar{\tau}$

Anomalous results had been obtained for the effect of temperature on the dielectric dispersion of filaments (see Fig. 2 in Gerber *et al.*, 1972). Therefore, electric birefringence decay data were obtained on solutions of flagellar filaments at temperatures between 16 and 36°C. Data were decomposed by computer into three terms and $\bar{\tau}$ was evaluated as described above.

Due to the effect of temperature on solvent viscosity, the relaxation time of macromolecules is expected to vary with temperature. When changes in solvent viscosity were considered, a linear relationship between $\bar{\tau}$ and η/T was obtained (Fig. 6). Furthermore, $\bar{\tau}$ appears to be independent of protein concentration since data obtained for two sets of filament solutions (0·39 and 3·08 mg/ml, open and filled circles in the Fig.) lie on the same line. Each point in the Figure is the average of six experiments. It is also worth noting that the least-squares line for the data passes through the origin ($\bar{\tau} = 0$, $T = \infty$).

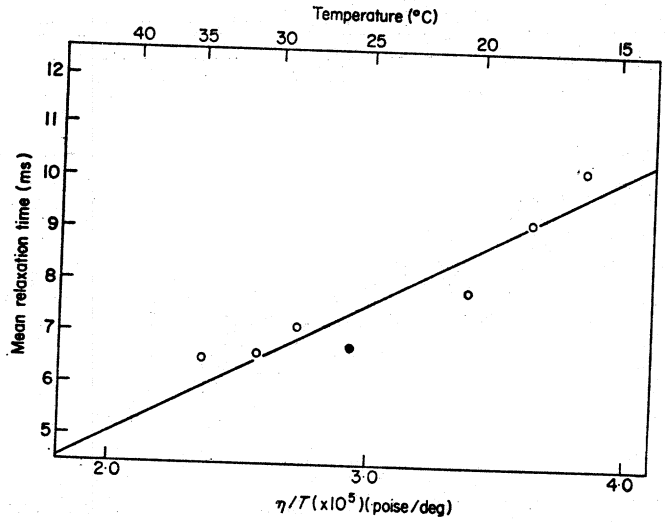

FIG. 6. Relation between mean relaxation time for short polymers $\bar{\tau}$ and the temperature and viscosity of the solvent. The abscissa incorporates the effect of changes in solvent viscosity (η) with temperature. Protein concentrations, 0·39 (○) and 3·08 (●) mg/ml.

The mean relaxation time was found to decrease with increase in the intensity of the applied field. Table 2 lists values for $\bar{\tau}$ in three ranges of field intensity and at various temperatures. In a polydisperse system O'Konski *et al.* (1959) and Yoshioka & Watanabe (1969) have shown that complete orientation of molecules produced by high field intensities leads to decay times corresponding to a weight average $\bar{\tau}$. Experiments done at low field intensities result in partial orientation of molecules and produce a $(Z + 1)$ average of $\bar{\tau}$. For instance, at low and high field intensity limits $\bar{\tau}$ can be calculated using equations (20) and (21) and the length distribution of short filaments determined with the electron microscope (see Discussion, section (d) and Fig. 10). These values are 5·8 ms at $E \to \infty$ and 16·3 ms at $E \to 0$. At 18°C the values of $\bar{\tau}$ obtained experimentally at 4·2 and 0·66 kV/cm, respectively, are 6·5 and 10·3 ms. (The ratio of $\bar{\tau}$ obtained at high and low field intensities can serve as a

TABLE 2

Relation between $\bar{\tau}$ and the range of applied field intensity (E) *at various temperatures*

Temperature (°C)	Mean relaxation time (ms) Field intensity (in V/cm) range $E < 10^3$	$10^3 < E < 2\times10^3$	$E > 2\times10^3$	Average value
16·1	10·4	10·8	9·0	10·3
18·0	10·7	9·7	8·1	9·2
20·5	10·9	7·4	6·6	7·9
25·9	—	7·3	5·7	6·8
28·8	9·0	7·1	5·7	7·1
31·2	7·7	7·0	6·1	6·6
34·8	9·0	6·5	5·3	6·5

measure of the polydispersity of the sample.) The trend of our results is in agreement with this proposal.

(f) *Cumulative electric field effects*

While determining whether electric birefringence was a destructive measurement or if samples could be reused we came across an interesting phenomenon.

Application of voltage pulses over long durations, e.g. 10 ms, caused a decrease in the steady-state birefringence of the sample. Similarly, the successive application of two or more brief pulses to the same sample solution resulted in the same effect. These phenomena were more remarkable at higher field intensities. A typical example is shown in Plate III where four pulses were applied for 5-ms durations at intervals of 11 ms. The decreases in optical gain (lower curved trace in the Plate) are obvious,

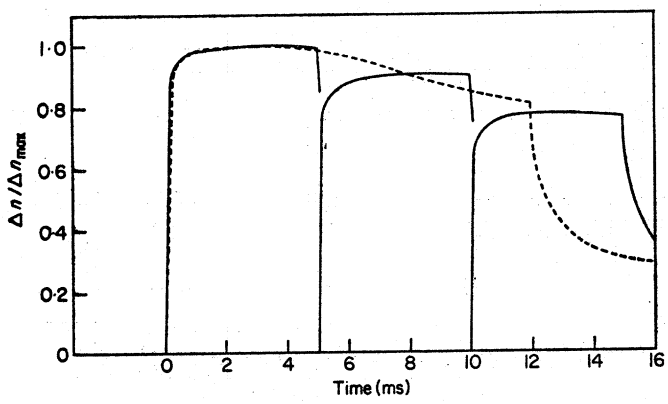

FIG. 7. Comparison of the effect of multiple pulses and an extended pulse on the electric birefringence of short polymers of flagellar filaments at 18°C. (- - - - - -), Shows the optic response of the solution to a single rectangular wave pulse. Applied field intensity, 3·91 kV/cm; $\Delta n_{max} = 6{\cdot}25\times10^{-6}$. (————) Shows optic response of the solution to three rectangular-wave voltage pulses. Pulse duration and the interval between pulses were 5 ms and 15 s. Intensity of the applied field and the Δn_{max} for the first pulse were 3·61 kV/cm and $5{\cdot}66\times10^{-6}$, respectively.

(e) *Deionized water*

Water of high purity was used to prepare solutions for electro-optical studies. By passing water from a single-stage distillation through a mixed bed Amberlite resin deionizing column (Continental Water Co., Philadelphia, Pa.) it was possible to obtain ion-free water with electrical conductivity less than 10^{-6} mho/cm. Between 16 and 28°C the pH of a solution of long or short polymers of flagella (3·4 mg/ml, w/v in ion-free water) was $6{\cdot}70 \pm 0{\cdot}03$.

(f) *Electron microscopy*

Specimens of freshly purified flagellar filaments or sonicated fragments of these were placed on carbon-coated formvar-covered copper grids (200 mesh, Mason & Morton, Ltd, England) and negatively stained with potassium phosphotungstate (2%, w/v, pH 7·0). Grids were examined in a Philips electron microscope (model 200) at an accelerating voltage of 60 kV. Instrumental magnification was calibrated with a carbon grating having 54,864 lines/in.

The size distribution of filaments was estimated from photographs at either $2{\cdot}4 \times 10^4$ or $4{\cdot}2 \times 10^4$ times magnification of the true dimensions of specimens. Both contour and end-to-end lengths of filaments were measured with a ruler scaled to resolve lengths greater than 0·02 μm with a precision of $\pm 3\%$.

(g) *Electric birefringence apparatus*

A schematic diagram of the apparatus used is shown in Fig. 1. The electric birefringence cell and the pulse-generating and detecting systems have been described in detail by Kahn & Wittnauer (1971) and Kahn (1972).

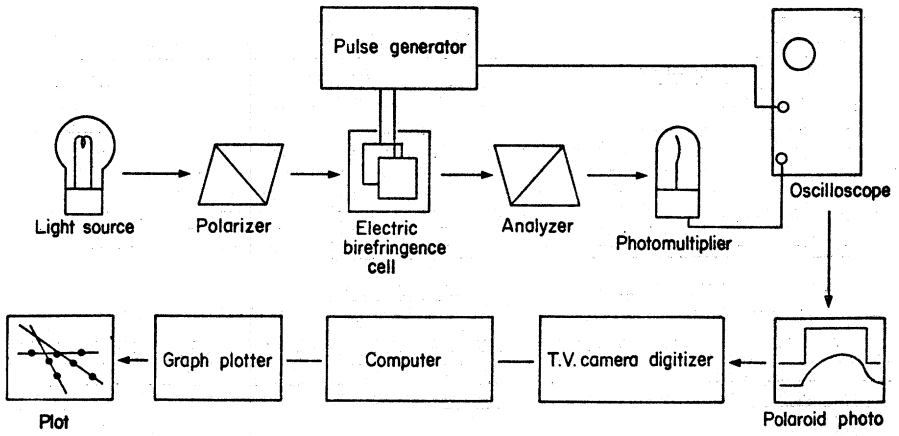

FIG. 1. Schematic illustration of the apparatus used for the production, measurement, display digitization and analysis of the birefringence of a polymer solution in an electric field.

Light from an incandescent bulb (type CPG projector lamp, $\lambda_{av} = 535$ nm, 100 W, General Electric Co.), powered by a d.c. power supply, was directed through an electric birefringence cell, a pair of polarizing (Rochon) prisms and a photomultiplier. All components were aligned on an optical bench. The birefringence cell was patterned after the design of O'Konski & Haltner (1956). It consisted of a quartz spectrophotometric cuvette with 10-mm light-path fitted with two flat parallel platinum sheet electrodes (area = 1 cm^2, spaced apart either 0·273 cm or 0·234 cm, thickness = 0·030 cm).The cuvette and electrodes were placed in a thermojacketed brass cell-holder through which water was circulated (Haake model F thermostat and pump) to maintain sample temperature within $\pm 0{\cdot}1$ deg. C. Experiments were done at temperatures between 16 and 35°C.

In the absence of an applied electric field the polarizing prisms, placed before and after the cell, were crossed so that no light passed to the photomultiplier. Subsequently, a

length distribution of filaments observed by electron microscopy. Finally, when multiple voltage-pulses or pulses of long duration were applied to solutions of filaments, the electric birefringence signal decreased to lower values. Analysis of birefringence after field cut-off indicated that mean lengths of filaments were unaffected by the application of electric fields. On the other hand, the time course for this phenomenon, as well as its dependence on field intensity and filament concentration, connotes that reversible side-by-side aggregation of filaments had been induced by electric fields. Since many biological filaments are in proximity to or embedded in membranes, this finding suggests the possibility that variations in membrane potential may influence filament and tubule interactions.

2. Materials and Methods

(a) *Bacterial cells*

Salmonella equi-abortus strain SJ25, used in this study, was a generous gift of Professor Tetsuo Iino, Laboratory of Genetics, University of Tokyo, Japan. In liquid media these cells undergo translational movements at a mean velocity near 75 μm/s at 22°C. In the late exponential phase of growth, each SJ25 cell has an average of 4 to 8 peritrichous flagella of H-antigen type 1·2. The pitch and diameter of helical flagella filaments are 2·4 μm and 200 Å (Plate I(a)).

(b) *Cultivation of cells*

Salmonella strain SJ25 cells were grown at 37°C with aeration in liquid media (5 l) containing 1% (w/v) yeast extract (Baltimore Biological Labs), 1% (w/v) peptone (Difco Labs), 0·5% (w/v) glucose, 0·002% (v/v) antifoam-B (Dow Corning) and buffered with 0·06 M-potassium phosphate, pH 8·0. After 6 to 8 h a population density of 10^9 cells/ml was attained and cells were harvested by centrifuging the media at 10,000 *g* for 20 min at 4°C. Unless noted otherwise subsequent procedures were done at 0 to 4°C.

(c) *Isolation and purification of flagellar filaments*

Pelleted cells were suspended in deionized water (2 vol.), mechanically shaken for 5 min and again centrifuged at 10,000 *g* for 20 min. The supernatant fluid, a solution of impure flagellar filaments, was slightly opalescent and slightly viscous. Filaments were pelleted as clear gels by centrifuging this solution at 78,000 *g* for 1 h.

Purification of flagellar filaments was achieved by differential centrifugation as described previously (Gerber *et al.*, 1973). Plate I(b) is an electron micrograph of purified flagellar filaments negatively stained with 2% (w/v) potassium phosphotungstate (analytical grade, Mallinckrodt, New York), pH 7·0. This material is referred to hereafter as *long polymers* of flagellar filaments.

(d) *Short polymers of flagellar filaments*

In a jacketed vessel cooled with circulating tap water, 15 to 25 ml of a solution of flagellar filaments (protein concn < 4 mg/ml) were fragmented with ultrasonic fields. Sonication was done twice for 15-s intervals at a nominal frequency of 2×10^4 cycles/s average power output of 75 W and a sonic "pressure" of 5·8 g. After standing 2 h at room temperature, solutions were centrifuged at 78,000 *g* for 1 h. Pelleted sonic fragments of the filaments were resuspended in deionized water to a final concentration of 3 to 8 mg/ml and stored at 0°C. Solutions were used within 2 weeks after preparation and no change in the physical properties of these filaments have been noted in this period of time. Plate I(c) is an electron micrograph of fragmented flagellar filaments negatively stained with 2% (w/v) potassium phosphotungstate, pH 7·0. This material is referred to subsequently as *short polymers* of flagellar filaments.

although small decreases in field intensity (upper short lines), presumably due to an increase in conductivity of the solution, are also observed.

Figure 7 compares the time course for decrease in Δn arising from voltage pulses of long duration (12 ms, $E = 3{\cdot}91$ kV/cm) and multiple pulses (each pulse duration = 5 ms, interval between pulses = 15 s, $E = 3{\cdot}61$ kV/cm). A decrease in applied field between successive pulses was sometimes observed. Corrections to Δn were made by using the relation between Δn and E^2 depicted in Figure 2. Since the field intensity is sufficient to fully orient the molecules within several milliseconds a secondary effect of the field appears responsible for the delayed decrease in Δn observed. In general the two curves are superposable and this indicates the correspondence in these cases for the cumulative effects of the applied field on the birefringence of flagellar filaments.

On applying multiple voltage pulses it was found that the first few pulses were most effective in decreasing Δn. On the other hand, after five or six pulses Δn remained unchanged indicating that this effect can be saturated. The field-induced decrease in Δn was reversible since recovery was observed when the time interval between pulses was five minutes; recovery did not occur, however, when the interval between pulses was two minutes or less. Hence the time constant for reversing this process was greater than two and less than five minutes.

To exclude the possibility that electrode polarization was responsible for the field-induced effect on the Δn of filaments, electrodes were manually reversed (≤ 4 s). Nevertheless, the same field-induced reduction in Δn was observed. Furthermore, this effect was strongly dependent on the intensity of the electric field. At 650 V/cm a decrease in Δn was not observed, whereas at 3·5 kV/cm the value of Δn falls to 60% of its initial value. The effect of field intensity in eliciting a decrease in Δn is summarized in Table 3.

TABLE 3

Electric birefringence of short polymers of flagellar filaments after multiple pulses at various field intensities†

Field intensity (kV/cm)	Values of Δn for 1st pulse ($\times 10^6$)	Relative birefringence‡ 2nd pulse	3rd pulse	4th pulse	5th pulse
0·65	2·78	1·0	1·0	1·0	—
0·80	3·25	0·99	0·99	0·97	—
1·64	3·92	0·95	0·91	0·86	0·81
2·79	4·98	0·95	0·85	0·82	—
3·45	4·64	0·88	0·71	0·64	0·63
3·61	5·66	0·91	0·78	0·78	0·76

† Protein concentration, 0·39 mg/ml; temperature, 18·0°C; duration of applied field, 5 ms.
‡ Birefringences are normalized to those values obtained on first voltage pulse, $\Delta n_i/\Delta n_1$.

Figure 8 shows the decrease in Δn obtained on application of a second and third pulse as a function of the protein concentration. At the lowest concentration studied (0·048 mg/ml), no decrease in Δn was observed. As the concentration increased, the relative value of Δn decreased by some power of the concentration higher than unity.

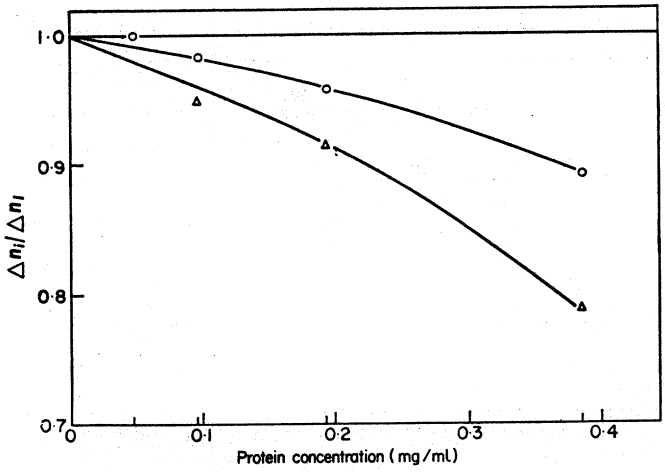

FIG. 8. Concentration dependence of the multiple pulse phenomenon. Ordinate represents relative values of Δn after second (○) and third (△) pulses. Pulse duration and applied field intensity are 12 ms and 1·62 kV/cm. Temperature, 18·0°C. Each point is the average value of two experiments which yielded close results. In one experiment the interval between pulses was 1 s, in the other it was 1·5 min.

This would indicate that the phenomenon is not related to an intramolecular process but rather to an intermolecular process such as the aggregation of filaments. The mode of aggregation is believed to be sidewise since no appreciable change in the relaxation time for the decay process was observed either after application of several voltage pulses or a single pulse of long duration. Therefore, the end-to-end lengths of filaments were not drastically altered by repeatedly pulsing the solution.

4. Discussion

Double refraction is produced when an electric field is applied to a solution of flagellar filaments which normally is optically isotropic. This phenomenon, referred to as the Kerr effect, is the result of the orienting effect of the electric field. From analysis of the time-dependence of electric birefringence, information is obtained on the optical and electrical properties, shape, mean size and size distribution of the filaments. Moreover, the finding that under specified conditions interactions between filaments and an electric field can produce long-lived filament–filament interactions may have broad biological implications.

(a) *Mechanism for orientation in an electric field*

Previously, interpretation of the dielectric dispersion by flagellar filaments was based on orientation of a *permanent dipole moment* in an oscillating electric field (Gerber *et al.*, 1972). It was conceded that data were few and obtained in a frequency region where experimental errors were large.

The findings in this electric birefringence study also indicate that alignment of flagellar filaments in the field is due primarily to orientation of a permanent dipole moment. (i) Reference to equation (11) shows that comparison of the shape of rise and decay curves may indicate the mode of molecular orientation by the field. For

example, if orientation is solely due to an induced dipole moment $b^2/2c = r = 0$. In this case, rise and decay curves will mirror each other and the ratio of areas represented by numerator and denominator A_1/A_2 in equation (11) will be one. Plate II(a) shows the time course for the rise curve (region I) to be considerably slower than the decay curve (region III); this is more pronounced at still lower field intensities. In fact, at field intensities of 429 and 235 V/cm, respectively, the ratio A_1/A_2 has the values 1·49 and 2·66. Yoshioka & Watanabe (1969) have shown that in the case of electric field orientation solely due to a permanent dipole moment, as $E \to 0$, $A_1/A_2 \to 4$. Clearly, the electric birefringence data for flagellar filaments show a tendency to approach this limiting value. (ii) The procedure devised by O'Konski *et al.* (1959), described briefly in Materials and Methods, section (i), permits estimation of the relative contributions of permanent and induced moments to orientation of molecules by the electric field. In Figure 9 values of $(\Delta n/E^2)/(\Delta n/E^2)_{E\to 0}$ obtained at temperatures between 16 and 35°C are graphed against log (E^2). Comparison with similar curves of the function $15\phi(\beta,\gamma)/(\beta^2 + 2\gamma)$ *versus* $\log(\beta^2 + 2\gamma)$ indicate that $\beta^2/2\gamma > 10$. The line between points in Figure 9 is the theoretical curve for the case where $\beta^2/2\gamma = \infty$, that is, purely permanent dipole moment orientation.

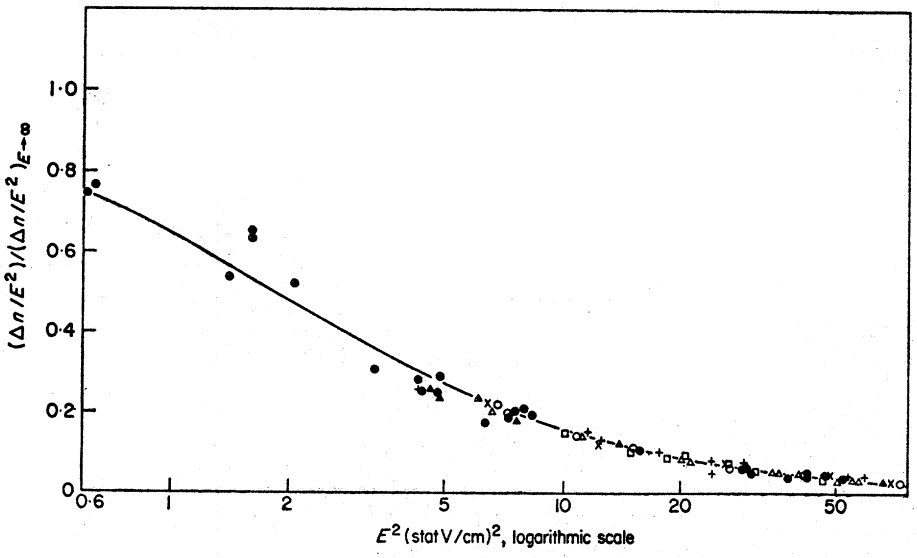

FIG. 9. Effect of applied field intensity on the relative electric birefringence of short polymers of flagellar filaments. Temperature (°C): (□) 16·1; (●) 18·0; (○) 20·5; (+) 25·9; (▲) 28·8; (△) 31·2; (×) 34·8. The theoretical curve for orientation due solely to a permanent dipole moment is included.

(b) *Evaluation of dipole moment*

The foregoing results encouraged us to evaluate μ for flagellar filaments by four procedures. The first one involved use of data in Figure 9 and determining the extent of translation along the abscissa required to give a best fit to one of the theoretical curves. A second procedure used equation (7) taking $c = 0$ and inserting the values of Δn obtained at limiting high and low field intensities. A third one used equation (8) due to O'Konski *et al.* (1959) which is valid for limiting high field intensities where orientation arises by permanent dipole moments. Finally, μ could be estimated

TABLE 4

Values of dipole moment obtained by several procedures

	Procedure used	Field intensity region required for Δn data	μ ($\times 10^{-4}$) (Debye units)
1.	Translation along abscissa in Fig. 9	Entire region (mainly low)	9·9
2.	Equation (7)	Limiting high and low field regions	9·6
3.	Equation (8)	Limiting high field region	6·6
4.	Equation (15)	Limiting high field region	14·2
		Average	10·1±2·7

from the time constants of the rise and decay curves (O'Konski *et al.*, 1959) with the use of equation (15). The method used, the field intensity region from which data were taken and the value of μ obtained are summarized in Table 4. The mean and standard deviation of μ are 10·1 ($\pm$ 2·7) $\times$ 10^4 Debye units. Analysis of the substructure of flagella by electron microscopy indicates that a filament has about 2×10^3 protomers per μm contour length (Routledge *et al.*, 1973) so that a filament with a mean contour length of 0·39 μm is composed of 780 flagellins. Therefore, the dipole moment per monomer in a filament is 129 ($\pm$ 35) Debye units which, in view of the different techniques used, compares favorably with the value of 140 ($\pm$ 25) Debye units obtained earlier from measurements of dielectric dispersion (Gerber *et al.*, 1972).

(c) *Electro-optical parameters*

Table 5 lists values of the electro-optical parameters and the relaxation times of flagellar polymers obtained in this study and, for comparative purposes, includes values reported previously for several other biological materials.

The specific Kerr constants are indicative of the relative response of a molecule to an applied electric field. The values of 6·14 and 11·1 $\times$ 10^{-3} e.s.u. for short and long polymers of flagellar filaments are among the largest reported for biopolymers. A further comparison can be made since equation (5) indicates that K_{sp} is proportional to μ^2 and hence to the square of the length (l) of filaments. The respective values of the ratio K_{sp}/L^2 for short and long polymers is 25·6 $\times$ 10^5 and 8·2 $\times$ 10^5 e.s.u./cm^2. Thus, per unit length, the K_{sp} of long polymers is smaller than the K_{sp} of short polymers.

The optical anisotropy factor directly reflects the degree of asymmetry of particles in solution. The values of $(g_1 - g_2)$ observed for flagellar filaments are in accord with published values obtained for other elongated biopolymers. Nevertheless, the order of $(g_1 - g_2)$ values for short and long flagellar polymers listed in Table 5 appears reversed. A possible explanation for this result is provided in Plate I(b) and (c). Although short filaments appear to be straight rods, longer filaments have pronounced curvature. On the assumption that a prolate ellipsoid of revolution can serve as model for both straight and curved filaments, a likely effect of introducing curvature to filaments would be to increase the molecular domain of filaments, reduce

TABLE 5

Values of electro-optical parameters of several biological macromolecules

Samples	Molecular weight ($\times 10^{-5}$)	$K_{sp} \times 10^5$ (e.s.u.)	$(g_1 - g_2) \times 10^3$	$\mu \times 10^{-4}$ (Debye units)	$(\alpha_1 - \alpha_2) \times 10^{15}$ (cm^3)	$\tau \times 10^5$ (s)	References
Flagella							
Short polymer	310	614	5·7	10·1		920	This work
Long polymer	720	1330	3·6	16·3		3600	This work
Flagellin	0·4			0·085		0·013	Kobayasi & Maruyama in Asakura (1970)
F-actin							
Short polymer	103	8·9	7·0	0·75		165	Kobayasi *et al.* (1964)
Long polymer	1100			2800		196,000	Kobayasi *et al.* (1964)
Collagen	2·8	4·3	1·7	1·5	2·7	15	Yoshioka & O'Konski (1966)
Fibrinogen	3·5	0·031	18	0·022		0·46	Tinoco (1955)
Tobacco mosaic virus	490	136	6·0		54	139	O'Konski *et al.* (1959)
T4B phage	1940	4·0	0·454	2·4	1·99	60	Greve & Blok (1973)
DNA	3·7	2200	7·1		1·32	4·9	Hornick & Weill (1971)

their apparent axial ratio, and, consequently, reduce the value of $(g_1 - g_2)$ observed. In this regard, Figure 4 showed that increases in temperature between 16 and 20°C had resulted in decreases in $(g_1 - g_2)$. Furthermore, the relaxation time of filaments, when corrected for the variation in solvent viscosity with temperature, indicated that no large change in the mean length of filaments had occurred (Fig. 6). The observed decrease in $(g_1 - g_2)$ between 16 and 20°C appears indicative of a reduction in the asymmetry of filaments and is consistent with the occurrence of thermally-induced increase in the flexibility of filaments.

(d) *Mean length and length distribution of filaments*

Semilogarithmic graphs of the relative birefringence remaining after cut-off of the electric field *versus* time were non-linear and indicated a distribution of relaxation times (Fig. 5(a)). Such results may sometimes be taken to indicate either that various *modes* of molecular relaxation can occur or that the sample is polydisperse. Plate I(b) and (c) clearly indicates that the samples were polydisperse and that the distribution in size of filaments is an important factor in the distribution of relaxation times observed.

To gain information on the size of the samples, birefringence decay data were decomposed by computer into weighted terms of equation (16). Computer simulations of the data indicated that they could be fitted well by a three-term expression (Fig. 5(b)) and that the ratio of apparent relaxation times for short polymers in solution was approximately 0·1:1:10. (In some instances, four-term decompositions were made successfully.) Data could be fit more quickly by maintaining the ratio of two "known" values for τ and permitting the computer to calculate a third value for τ which yielded the best fit to the data. Moreover, it was found that the third value calculated satisfied the decade ratio of relaxation times. (In all cases the aforementioned criteria for defining an acceptable solution by computer were applied.) It was soon apparent that the same data could be fit by various three-term expressions although their relative contributions would differ. This suggested that the distribution in relaxation times might be graphically synthesized by superposing the contribution of each term against its relaxation time.

To permit comparison with the size distribution of filaments visualized by electron microscopy, 14 computed values of τ were converted to lengths of their equivalent ellipsoids of revolution with the use of equation (19) due to Perrin (1934). Each calculated length was taken to represent the mean of a normal distribution in lengths around the calculated value. Therefore, with $\sigma = 0{\cdot}1$ μm the Gaussian distribution for each calculated length was determined. Finally, a composite length distribution curve was produced by summing the 14 Gaussian distributions of calculated lengths. In Figure 10 the length distribution curve of short polymers of flagellar filaments determined by computer decomposition of electric birefringence decay data is compared with the end-to-end length distribution histogram determined by electron microscopy. Since birefringence data at high field intensity are referred to the volume concentration of constituents, the ordinate in Figure 10 is given in terms of $\nu_i l_i$, which expresses concentration, rather than in ν_i alone. The value of χ^2 for agreement of the two distributions at mid-interval lengths is 0·078 with seven degrees of freedom. This corresponds to a confidence limit better than 99% and indicates an excellent fit of the two distributions.

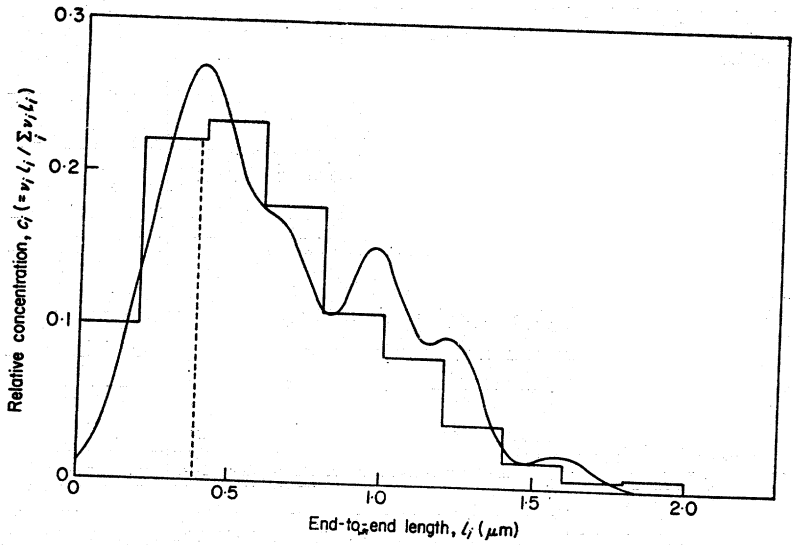

FIG. 10. Comparison of size distribution of short polymers determined by electron microscopy and computer analysis of the electric birefringence decay curve. Histogram is the electron microscopy data. Number of filaments sampled was 657. Mean length (dashed vertical line); standard deviations were 0·39 and 0·31 μm. Continuous curve is the sum of normal length distributions calculated from values of apparent relaxation time due to computer analysis of birefringence decay process. Experimental conditions were identical to those cited in Table 1. Calculated mean end-to-end length was 0·49 μm. See text for details.

(e) *Field-induced effects*

Electric fields had a cumulative effect in decreasing the birefringence of flagellar filaments (Plate III). On standing five minutes the decrease in Δn was quantitatively reversed for short polymers but appeared to be only partly reversed for long polymers. (It is possible that full reversal for long polymer samples requires longer times.) The phenomenon proved to be a function of filament concentration (Fig. 8) and the duration and intensity of the applied field (Table 3). Decreases in Δn were not observed if solutions were too dilute (filament concn $<0{\cdot}05$ mg/ml) or if the intensity of the applied field was too low ($E < 0{\cdot}8$ kV/cm). Dependence of this phenomenon on filament concentration excludes as an explanation any role of intramolecular interactions. In addition, the observed decreases in Δn were produced quickly, within several milliseconds after impulse, whereas a relatively long time was required, several minutes, for reversal of this effect. Thus the ratio for the two times was about 10^4.

Reversing the polarity of the electrodes in the midst of the phenomenon had no measurable effect and so the field-induced reduction in Δn was not due to polarization of the electrodes. Furthermore, within experimental limits, the mean relaxation time (and mean length) of filaments remained unchanged between voltage pulses. Equations (19) to (21) show τ to be proportional to l^3 but relatively less sensitive to changes in the diameter and axial ratio of molecules. Evidently, this effect was not due to scission of filaments by the electric field.

We interpret these results to indicate that side-by-side aggregation of filaments was produced by electrical impulses of sufficient intensity and duration. Field-induced molecular aggregations and dissociations have been described by Neumann

& Katchalsky (1972) and Jennings and coworkers (Riddiford & Jennings, 1967; Brown & Jennings, 1973). Such inter- and intramolecular interactions are thought to occur from perturbations by the field of the ionic atmosphere of the molecules. This may then promote attractions between zwitterion species, such as proteins, or repulsions between polyions of like charge, such as RNA. As a result, either aggregation, strand-separation or dissociation may occur. Alternatively, the electric field may affect the structure of the filament causing bends and curves to form. This might alter the dipole moment and promote filament–filament interactions.

(f) *Permanent dipole moments, protein filaments and bacterial motility*

Permanent dipole moments appear to be relevant factors in the self-assembly of proteins and perhaps in the motility of bacteria. It was found earlier (Gerber *et al.*, 1972) that flagellin monomers, as well as other proteins capable of self-assembly, have remarkably large permanent dipole moments. The magnitude of the moment falls considerably on *in vitro* polymerization of these proteins. Since μ is a vector quantity, it was suggested that neutralization of permanent dipole moments may dictate the morphology of the polymer and/or the rate of its assembly.

In addition, the electric properties of flagellar filaments may be incorporated in aspects of the mechanism for bacterial movement. For example, these and other biological filaments are in proximity to cell membranes across which the electric potential may exceed 10^6 V/cm. As shown by their large values of K_{sp}, flagellar filaments are highly responsive to electric fields. It follows that variations in potential along the surface of the membrane of merely 10^3 V/cm would serve to orient flagella with respect to the cell surface. Moreover, changes in potential of sufficient intensity and duration can induce long-lived sidewise aggregation of flagella to bundles. The formation of flagella bundles has been described both on cells in motion (Pijper, 1957; Macnab & Koshland, 1974) and for isolated filaments (Mitani & Iino, 1968). This phenomenon may be particularly important for organisms with peritrichous flagellation. For the production of bundles would serve to co-ordinate the activity of bacterial flagella and, in addition, would produce stronger structures.

We thank Dr Martin Pring for providing a computer program to analyze our data and Mrs Doris Bush for expert technical assistance in electron microscopy. We also thank Dr Ralph O. Erickson for stimulating discussions and Dr Lewis M. Routledge for assistance in the early phase of this work. Support of this study by the National Science Foundation, grant GB38348, and the National Institutes of Health, Biotechnology grant RR15, is acknowledged with gratitude.

A preliminary report of this work was made at the session on "Self-associating Systems", 18th Annual Meeting of the Biophysical Society on 3 June 1974, in Minneapolis, Minnesota.

REFERENCES

Asakura, S. (1970). *Advan. Biophys.* **1**, 99–155.
Benoit, H. (1951). *Ann. Phys.* **6**, 561–609.
Brown, B. L. & Jennings, B. R. (1973). *J. Colloid Interface Sci.* **43**, 170–175.
Gerber, B. R. & Noguchi, H. (1967). *J. Mol. Biol.* **26**, 197–210.
Gerber, B. R., Routledge, L. M. & Takashima, S. (1972). *J. Mol. Biol.* **71**, 317–337.
Gerber, B. R., Asakura, S. & Oosawa, F. (1973). *J. Mol. Biol.* **74**, 467–487.
Gornall, A. G., Bardawill, A. J. & David, M. M. (1949). *J. Biol. Chem.* **177**, 751–766.
Greve, J. & Blok, J. (1973). *Biopolymers*, **12**, 2607–2622.
Holtzman, E. (1974). *Hosp. Pract.* **9**, 75–88.

Hornick, C. & Weill, G. (1971). *Biopolymers*, **10**, 2345–2358.
Iino, T. (1969). *Bacteriol. Rev.* **33**, 454–475.
Kahn, L. D. (1972). In *Methods in Enzymology* (Colowick, S. P. & Kaplan, N. O., eds), vol. 26, pp. 323–337, Academic Press, New York & London.
Kahn, L. D. & Wittnauer, L. P. (1971). *Biochim. Biophys. Acta*, **243**, 388–397.
Kobayasi, S., Asai, H. & Oosawa, F. (1964). *Biochim. Biophys. Acta*, **88**, 528–540.
Kushner, D. J. (1969). *Bacteriol. Rev.* **33**, 302–345.
Macnab, R. & Koshland, D. E. (1974). *J. Mol. Biol.* **84**, 399–406.
Matsumoto, M., Watanabe, H. & Yoshioka, K. (1970). *Biopolymers*, **9**, 1307–1317.
Mitani, M. & Iino, T. (1968). *J. Gen. Microbiol.* **50**, 459–464.
Neumann, E. & Katchalsky, A. (1972). *Proc. Nat. Acad. Sci., U.S.A.* **69**, 993–997.
O'Konski, C. T. & Haltner, A. J. (1956). *J. Amer. Chem. Soc.* **78**, 3604–3610.
O'Konski, C. T. & Haltner, A. J. (1957). *J. Amer. Chem. Soc.* **79**, 5634–5649.
O'Konski, C. T., Yoshioka, K. & Orttung, W. H. (1959). *J. Phys. Chem.* **63**, 1558–1565.
Perrin, F. (1934). *J. Phys. Radium*, **5**, 497–511.
Peterlin, A. & Stuart, H. A. (1939). *Z. Physik*, **112**, 129–147.
Pijper, A. (1957). *Ergebn. Mikrobiol. Immun. Forsch. exp. Ther.* **30**, 37–95.
Riddiford, C. L. & Jennings, B. R. (1967). *Biopolymers*, **5**, 757–771.
Routledge, L. M., Gerber, B. R. & Erickson, R. O. (1973). *Biophys. J. Soc. Abst.* **13**, 1582.
Schwan, H. P. (1963). In *Physical Techniques in Biological Research* (Nastuk, W. L., ed.), vol. 6, pp. 323–407, Academic Press, New York & London.
Tinoco, I. (1955). *J. Amer. Chem. Soc.* **77**, 3476–3480.
Yoshioka, K. & O'Konski, C. T. (1966). *Biopolymers*, **4**, 499–507.
Yoshioka, K. & Watanabe, H. (1969). In *Physical Principles and Techniques of Protein Chemistry, Part A* (Leach, S. J., ed.), pp. 335–367, Academic Press, New York & London.